Chapter 1

Gamma Decay

"Gamma radiation is the electromagnetic de-excitation of the nucleus: same species, lower energy, multipole selection rules, and competition from internal conversion."
nuclear-structure perspective [6, 1]

Alpha and beta decay change the nuclear identity (Z and/or A). **Gamma decay** does not: the same nucleus drops from an excited state to a lower level by emitting a photon. Excited states are populated most often by preceding β or α decay (or by nuclear reactions). The transition energy is typically tens of keV to a few MeV. This chapter develops multipole classification (EL, ML), the long-wavelength expansion, angular-momentum and parity selection rules, transition strengths and widths, angular correlations, and competition with internal conversion, following Krane, Dunlap, Basdevant, and Demtröder [6, 1, 14, 2, 32].

1.1 De-excitation energy and three standard sources

For a transition between two states of the same nuclide,

$$ {}^{A}_{Z}X^{*}(J_i^{\pi_i}) \longrightarrow {}^{A}_{Z}X(J_f^{\pi_f}) + \gamma, \tag{1.1} $$

neither A nor Z changes. The level spacing $E_0 = E_i - E_f$ is shared by the photon and the recoil of the final nucleus, so E_γ is slightly smaller than E_0. Excited states may be fed by alpha or beta decay, electron capture, inelastic scattering, or a capture reaction; the subsequent photon cascade reveals the daughter level scheme [6, 1].

1.1.1 ^{137}Cs: a line accompanied by conversion electrons

About 94.6% of ^{137}Cs beta decays feed the 661.7 keV, $11/2^-$ isomer of ^{137}Ba, whose half-life is 2.55 min. Its decay to the $3/2^+$ ground state has $\Delta J = 4$ and changes parity, so the leading photon multipole is $M4$ (the next allowed order is $E5$). The high order explains the isomerism and also makes internal conversion appreciable. A BrIcc calculation for $Z = 56$, $E_{\mathrm{tr}} = 661.7\,\mathrm{keV}$, pure $M4$, gives an illustrative total coefficient $\alpha_T \simeq 0.11$, hence $f_\gamma = 1/(1+\alpha_T) \simeq 0.90$. The exact coefficient used in an analysis must state the BrIcc atomic-vacancy convention and be checked against the evaluated transition record [6, 20, 21, 34].

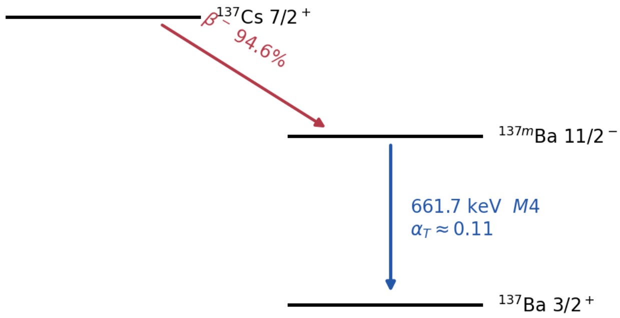

Figure 1.1: The ^{137}Cs decay scheme, showing the dominant beta feeding of the 661.7 keV ^{137}Ba isomer. Evaluated values should be taken from ENSDF/NuDat rather than read from this schematic [20, 21].

1.1.2 ^{60}Co: an ordered two-photon cascade

^{60}Co beta decay strongly populates the 2.505 MeV, 4^+ state of ^{60}Ni. Energy subtraction fixes the order of the cascade:

$$2.505\,\text{MeV}\,(4^+) \xrightarrow[E_\gamma=2.505-1.332]{1.173\,\text{MeV}\,(E2)} 1.332\,\text{MeV}\,(2^+) \xrightarrow[E_\gamma=1.332-0]{1.332\,\text{MeV}\,(E2)} 0\,(0^+). \tag{1.2}$$

The raw lecture prose interchanged these two photon assignments; the level differences above give the corrected ordering. The $2^+ \to 0^+$ leg is forced to be pure $E2$. The $4^+ \to 2^+$ leg permits $E2, M3, E4, \ldots$; it is conventionally treated as overwhelmingly $E2$, but "pure" is an experimental qualification, not a consequence of $\Delta J = 2$ alone. In particular this cascade is not the standard adjacent-order $M1 + E2$ mixing case. Its directional correlation is useful in coincidence experiments [6, 1].

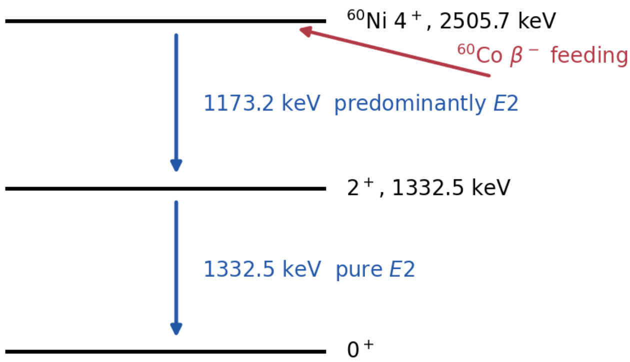

Figure 1.2: Partial ^{60}Co $\to$ ^{60}Ni decay scheme. The printed labels are 1.1732 and 1.3325 MeV; rounded values are used in the text.

1.1.3 ^{22}Na: nuclear and annihilation photons

^{22}Na decays mainly by positron emission, with a smaller electron-capture branch, to the 1.274 MeV state of ^{22}Ne. Its de-excitation photon is therefore observed together with two 511 keV annihilation photons from the positron. The 1.274 MeV line is nuclear; the 511 keV lines are annihilation radiation [6, 20].

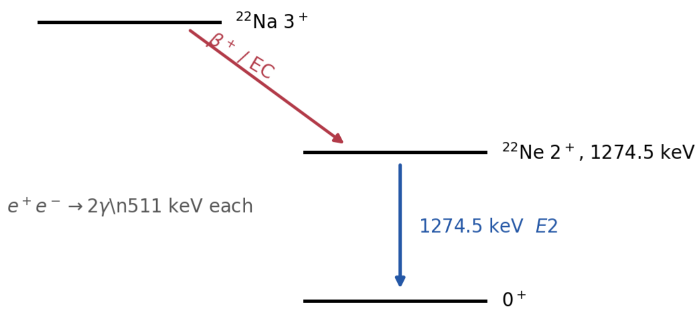

Figure 1.3: The ^{22}Na decay scheme. Branch percentages are retained as lecture-level rounded values; ENSDF is the authority for evaluated intensities [20].

Gamma ray or X-ray? The names identify origin, not a non-overlapping energy range. A gamma ray comes from nuclear levels; an X-ray comes from an electronic-shell vacancy. Consequently a low-energy gamma ray may have less energy than a hard X-ray [1, 2].

1.2 From a localized source to electromagnetic multipoles

Let the transition frequency be $\omega = E_\gamma/\hbar$, the photon wave number $k = \omega/c$, and the nuclear radius $R \simeq 1.2A^{1/3}$ fm. The expansion parameter is

$$kR = \frac{E_\gamma R}{\hbar c} \simeq 6.08 \times 10^{-3} A^{1/3} \left(\frac{E_\gamma}{\mathrm{MeV}}\right). \tag{1.3}$$

For $A = 100$ and $E_\gamma = 1\,\mathrm{MeV}$, $kR \simeq 0.028$. Thus the wavelength is long compared with the source, and the plane-wave factor can be ordered as

$$e^{i\mathbf{k}\cdot\mathbf{r}} = 1 + i\mathbf{k}\cdot\mathbf{r} - \frac{(\mathbf{k}\cdot\mathbf{r})^2}{2!} + \cdots. \tag{1.4}$$

After separating the angular dependence into scalar and vector spherical harmonics, successive terms are electric or magnetic multipoles. Their amplitudes contain powers of kR, and their rates contain E_γ^{2L+1}; this is the dynamical origin of the strong suppression of high L [6, 1, 2].

1.2.1 Long-wavelength operators

With the standard spherical-harmonic normalization, the leading electric operator is

$$\mathcal{M}(EL, M) = \int d^3r\, \rho(\mathbf{r})\, r^L Y_{LM}(\hat{\mathbf{r}}) \simeq e \sum_{p=1}^{Z} r_p^L Y_{LM}(\hat{\mathbf{r}}_p). \tag{1.5}$$

Only protons appear in the one-body charge form, although collective motion and effective charges can make the matrix element a property of many nucleons. A convenient current-density form of the magnetic operator is

$$\mathcal{M}(ML, M) = -\frac{i}{c}\sqrt{\frac{L}{L+1}} \int d^3r\, r^L\, \mathbf{Y}_{LLM}(\hat{\mathbf{r}}) \cdot \mathbf{j}(\mathbf{r}), \tag{1.6}$$

up to the conventional overall phase. For $M1$, its familiar one-body limit is

$$\mathcal{M}(M1, M) = \sqrt{\frac{3}{4\pi}}\, \mu_N \sum_a \big(g_{\ell,a}\boldsymbol{\ell}_a + g_{s,a}\mathbf{s}_a\big)_M. \tag{1.7}$$

Equations (1.5) and (1.6) also make the parity transparent: ρ is a scalar, $\mathbf{j}$ is a polar vector, and $\mathbf{r} \times \mathbf{j}$ is axial.

Why no single-photon $E0$ radiation? For $L = 0$, $\mathcal{M}(E0)$ begins with the conserved total charge. A radial pulsation may alter the charge distribution inside the nucleus, but outside it the monopole field remains a static Coulomb field; no transverse $1/r$ radiation field results. There is likewise no $M0$ moment in ordinary electrodynamics. A nuclear $E0$ transition can nevertheless couple directly to an atomic electron or, above threshold, create an e^-e^+ pair [6, 14].

1.3 Angular momentum, parity, and multipole mixing

A radiation multipole of rank L transfers angular momentum $L\hbar$. The Wigner–Eckart theorem gives the same triangle condition as vector addition:

$$|J_i - J_f| \le L \le J_i + J_f, \qquad L = 1, 2, 3, \ldots. \tag{1.8}$$

The lower bound is therefore

$$L_{\min} = \max(1, |J_i - J_f|) \tag{1.9}$$

provided $J_i + J_f \ge 1$. It is incorrect to replace (1.8) by the oversimplified statement $\Delta J = L$: for example, a $2 \to 2$ transition may contain $L = 1, 2, 3, 4$. If either endpoint has $J = 0$, however, the triangle collapses to a single value $L = J_{\text{nonzero}}$.

For $J_i = J_f = 0$, the triangle permits only $L = 0$, while a real single photon requires $L \ge 1$:

$$0 \longrightarrow 0 \quad \Rightarrow \quad \text{single-photon emission is forbidden.} \tag{1.10}$$

This statement applies to any $0 \to 0$ pair of parities, not just $0^+ \to 0^+$.

The parity carried by the two families is

$$EL: \quad \pi_f = \pi_i(-1)^L, \tag{1.11}$$

$$ML: \quad \pi_f = \pi_i(-1)^{L+1}. \tag{1.12}$$

Thus parity changes for $E1, M2, E3, M4, \ldots$, and is unchanged for $M1, E2, M3, E4, \ldots$. For each allowed L, parity selects one of EL or ML. Adjacent allowed orders may both occur: a same-parity $\Delta J = 1$ transition can be $M1 + E2$, whereas an opposite-parity one can be $E1 + M2$. Such a transition is not "half electric and half magnetic"; its amplitudes must be measured.

Remark

Assignment algorithm: (1) list every integer L satisfying (1.8), excluding $L = 0$; (2) apply (1.11)–(1.12); (3) compare the lowest one or two surviving multipoles using rates, angular correlations, polarization, or conversion coefficients. "Allowed" does not mean "equally probable" [6, 1].

1.4 Transition strengths, Weisskopf units, lifetimes, and widths

For an operator $\mathcal{M}(\sigma L)$, $\sigma = E, M$, define the reduced transition probability

$$B(\sigma L; J_i \to J_f) = \frac{1}{2J_i + 1} \left| \langle J_f \| \mathcal{M}(\sigma L) \| J_i \rangle \right|^2 . \tag{1.13}$$

For electric radiation, if $B(EL)$ is quoted numerically in $e^2\mathrm{fm}^{2L}$, the radiative decay constant is

$$\lambda_\gamma(EL) = \frac{8\pi(L+1)}{L[(2L+1)!!]^2} \left(\frac{E_\gamma}{\hbar c}\right)^{2L+1} \frac{e^2}{4\pi\epsilon_0\hbar} \frac{B(EL)}{e^2}. \tag{1.14}$$

The dimensions are explicit: $(E_\gamma/\hbar c)^{2L+1}$ contributes $\mathrm{fm}^{-(2L+1)}$, $(e^2/4\pi\epsilon_0)(B/e^2)$ contributes $\mathrm{MeV\,fm}^{2L+1}$, and division by $\hbar$ leaves s^{-1}. Magnetic rates have the same E_γ^{2L+1} dependence when $B(ML)$ is defined with the magnetic operator; magnetic strengths are conventionally reported in $\mu_N^2\mathrm{fm}^{2L-2}$ [6, 1].

1.4.1 The Weisskopf benchmark

The single-particle estimate replaces detailed wave functions by a uniform radial amplitude inside $R = 1.2A^{1/3}$ fm. The radial matrix element of r^L against a constant density is

$$\frac{\displaystyle\int_0^R r^L\, r^2\, \mathrm{d}r}{\displaystyle\int_0^R r^2\, \mathrm{d}r} = \frac{\displaystyle\int_0^R r^{L+2}\, \mathrm{d}r}{R^3/3} = \frac{3}{L+3} R^L. \tag{1.15}$$

Squaring and attaching the conventional angular-average factor $1/(4\pi)$ produces the electric Weisskopf unit. For magnetic radiation the single-nucleon current supplies a moment of order μ_N, while a rank L operator supplies R^{L-1}. In the conventional Weisskopf prescription the reduced single-particle estimate is

$$|\langle \mathcal{M}(ML) \rangle_{\mathrm{W}}| = \sqrt{\frac{10}{\pi}}\, \frac{3}{L+3} R^{L-1} \mu_N.$$

Squaring it (with the reduced-probability spin average understood) produces the magnetic expression below. Thus the conventional Weisskopf units are

$$B_{\mathrm{W}}(EL) = \frac{1}{4\pi} \left(\frac{3}{L+3}\right)^2 R^{2L}\, e^2, \tag{1.16}$$

$$B_{\mathrm{W}}(ML) = \frac{10}{\pi} \left(\frac{3}{L+3}\right)^2 R^{2L-2}\, \mu_N^2. \tag{1.17}$$

A measured strength is then stated as B/B_{W} in Weisskopf units (W.u.). This is a scale, not a precision prediction: configuration changes can hinder a transition, while coherent collective motion can enhance $E2$ strengths far above one W.u. [6, 1, 14].

Substitute $B_{\mathrm{W}}(EL)$ into the multipole rate (1.14) (with $R = r_0 A^{1/3}$, $r_0 = 1.2\,\mathrm{fm}$) and restore conventional units for E_γ in MeV. For the leading electric dipole case $L = 1$,

$$\lambda_{\mathrm{W}}(E1) \propto E_\gamma^3\, B_{\mathrm{W}}(E1) \propto E_\gamma^3\, R^2 \propto A^{2/3} E_\gamma^3, \tag{1.18}$$

and the numerical prefactor evaluates to $1.02 \times 10^{14}\, A^{2/3} E_\gamma^3$ (in s^{-1}). Higher multipoles bring higher powers of E_γ and of R (hence of A). The resulting internally consistent set of rough rates, with E_γ in MeV and λ_{W} in s^{-1}, is:

L	$\lambda_{\mathrm{W}}(EL)$	$\lambda_{\mathrm{W}}(ML)$
1	$1.02 \times 10^{14} A^{2/3} E_\gamma^3$	$3.15 \times 10^{13} E_\gamma^3$
2	$7.28 \times 10^{7} A^{4/3} E_\gamma^5$	$2.24 \times 10^{7} A^{2/3} E_\gamma^5$
3	$33.9 A^{2} E_\gamma^7$	$10.4 A^{4/3} E_\gamma^7$
4	$1.07 \times 10^{-5} A^{8/3} E_\gamma^9$	$3.27 \times 10^{-6} A^{2} E_\gamma^9$

At fixed A and E_γ, each increase in L is usually a severe penalty; in medium and heavy nuclei an EL Weisskopf rate is often roughly two orders of magnitude above the corresponding ML rate. The memorable 10^{-5} and 10^{2} rules are therefore only order-of-magnitude summaries, not constants independent of A, E_γ, or structure [6, 1].

1.4.2 From a rate to a line width

For a level with independent exit channels c,

$$\lambda_{\mathrm{tot}} = \sum_c \lambda_c, \qquad \tau = \lambda_{\mathrm{tot}}^{-1}, \qquad t_{1/2} = \tau \ln 2, \qquad \Gamma = \hbar \lambda_{\mathrm{tot}} = \frac{\hbar}{\tau}. \tag{1.19}$$

Here Γ is the full natural width in energy units and $\hbar = 6.5821196 \times 10^{-16}\,\mathrm{eV\,s}$. A branching fraction is $b_c = \lambda_c/\lambda_{\mathrm{tot}} = \Gamma_c/\Gamma$. Long lifetime means narrow natural width. High-L, low-energy, or structurally hindered transitions may produce metastable nuclear isomers [6, 1, 14].

1.5 Angular distributions and gamma–gamma correlations

An ensemble with equally populated magnetic substates has no preferred axis, so its single-photon distribution is isotropic even though each multipole has nontrivial angular structure. An anisotropy appears when the initial spins are aligned, or when detecting a first photon γ_1 in a cascade selects an unequal population of substates in the intermediate level. Relative to the γ_1 direction, the second photon has

$$W(\theta) = 1 + \sum_{\substack{k=2 \\ k\ \mathrm{even}}}^{k_{\max}} A_k P_k(\cos\theta). \tag{1.20}$$

The coefficients depend on the three spins, the multipole orders, detector acceptance, and any attenuation before the second decay. Odd Legendre terms are absent for the usual unpolarized electromagnetic cascade [6, 2].

For adjacent allowed multipoles, such as $M1 + E2$, the reduced matrix elements in Eq. (1.13) cannot be divided directly: they carry different electromagnetic dimensions. Define instead the dimensionless *radiation-amplitude* mixing ratio

$$\delta = \frac{\mathcal{A}(E2; J_i \to J_f)}{\mathcal{A}(M1; J_i \to J_f)}, \tag{1.21}$$

where each $\mathcal{A}(\sigma L)$ includes the multipole-dependent radiation normalization and its power of $E_\gamma/\hbar c$. Equivalently, $|\delta|^2 = \lambda_\gamma(E2)/\lambda_\gamma(M1)$ when interference has been removed by angular integration. The sign depends on the adopted phase convention and must be reported with it. After angular integration the idealized fractions are $f_{E2} = \delta^2/(1+\delta^2)$ and $f_{M1} = 1/(1+\delta^2)$, while the sign of δ remains visible through interference in A_k. Angular correlations determine L and mixing; linear polarization is needed to distinguish electric from magnetic character when angular distributions alone are degenerate [6].

1.6 Worked multipole assignments

1.6.1 ^{72}Ge: $0^+ \to 0^+$ and $2^+ \to 0^+$

Germanium-72 has a 0^+ ground state, a 0^+ first excited state at 691 keV ($t_{1/2} = 0.42\,\mu$s), and a 2^+ state at 834 keV ($t_{1/2} = 3.1$ ps).

$0^+ \to 0^+$ at 691 keV. Here $J_i = J_f = 0$, so (1.8) forces $L = 0$. No photon multipole exists. Gamma emission is forbidden. The state still decays by **internal conversion** (Section 1.7): the nuclear transition energy is transferred to an atomic electron [6, 1].

$2^+ \to 0^+$ at 834 keV.

$$|2 - 0| \le L \le 2 + 0 \quad \Rightarrow \quad L = 2. \tag{1.22}$$

Both states have positive parity, so $\pi_f = \pi_i$. For $L = 2$, electric radiation satisfies $\pi_f = \pi_i(-1)^2 = \pi_i$. The transition is pure $E2$. The short half-life is consistent with a low multipole order [6].

1.6.2 ^{117}In: large ΔJ

An excited state of ^{117}In at 315 keV has $J^\pi = \frac{1}{2}^-$; the ground state is $\frac{9}{2}^+$. Then

$$\left|\tfrac{1}{2} - \tfrac{9}{2}\right| \le L \le \tfrac{1}{2} + \tfrac{9}{2} \quad \Rightarrow \quad L = 4 \text{ or } 5. \tag{1.23}$$

Parity *changes* ($- \to +$).

- For $L = 4$: magnetic parity rule $\pi_f = \pi_i(-1)^5 = -\pi_i$ matches a change. Allowed multipole: $M4$.

- For $L = 5$: electric rule $\pi_f = \pi_i(-1)^5 = -\pi_i$ also matches. Allowed multipole: $E5$.

The extra power of $E_\gamma R/\hbar c$ makes $E5$ much slower than $M4$ on the Weisskopf scale despite the usual electric-over-magnetic advantage at equal L. The leading assignment is therefore $M4$; its high order explains the isomeric lifetime [6, 1].

Assign multipolarity for $3^- \to 0^+$

Possible L: $|3-0| \le L \le 3$, so $L = 3$. Parity changes. Electric $E3$ has $\pi_f = \pi_i(-1)^3 = -\pi_i$. Magnetic $M3$ would not change parity. Result: pure $E3$.

1.7 Internal conversion

1.7.1 Mechanism

In **internal conversion** (IC) the nuclear transition field ejects an electron already present in the atom. This is a single quantum process, not gamma emission followed by photoelectric absorption. Inner-shell wave functions have the greatest nuclear overlap, so K, L, and M conversion are especially important. For conversion from shell s,

$$K_{e,s} = E_{\mathrm{tr}} - B_s - E_{\mathrm{rec},e} \simeq E_{\mathrm{tr}} - B_s, \tag{1.24}$$

provided $E_{\mathrm{tr}} > B_s$. Different shell binding energies therefore produce discrete conversion-electron lines. The vacancy subsequently gives characteristic X-rays or Auger electrons; these atomic emissions should not be confused with the nuclear transition itself [6, 1, 2].

1.7.2 Conversion coefficient

Define partial decay constants λ_γ and λ_{IC} for photon emission and internal conversion. The **internal conversion coefficient** is

$$\alpha \equiv \frac{\lambda_{\mathrm{IC}}}{\lambda_\gamma} = \frac{N_e}{N_\gamma}, \tag{1.25}$$

with N_e and N_γ the numbers of conversion electrons and photons in the same transition after efficiency and fluorescence corrections. One also defines shell coefficients α_K, α_L, ... with $\alpha = \alpha_K + \alpha_L + \cdots$. The total electromagnetic width is

$$\lambda_{\mathrm{em}} = \lambda_\gamma + \lambda_{\mathrm{IC}} = \lambda_\gamma(1+\alpha), \qquad \Gamma_{\mathrm{em}} = \hbar\lambda_{\mathrm{em}}. \tag{1.26}$$

Consequently

$$f_\gamma = \frac{1}{1+\alpha}, \qquad f_{\mathrm{IC}} = \frac{\alpha}{1+\alpha}, \qquad \lambda_\gamma = \frac{\ln 2}{t_{1/2}(1+\alpha)} \tag{1.27}$$

for a level whose only decay is this one electromagnetic transition. With several branches j, one instead sums $\lambda_{\mathrm{level}} = \sum_j (1+\alpha_j)\lambda_{\gamma j}$. This correction is essential before inferring $B(\sigma L)$ from a measured level lifetime. Conversion grows with Z, falls rapidly with transition energy, and generally becomes more important at high multipole order [6, 1, 14].

1.7.3 $0^+ \to 0^+$: conversion only

For $0^+ \to 0^+$, $\lambda_\gamma = 0$ for single-photon emission. Below the pair threshold, the ordinary electromagnetic channel is $E0$ internal conversion. Internal pair formation opens at $E_{\text{tr}} > 2m_ec^2 = 1.022\,\text{MeV}$. Because the reference photon rate vanishes, the usual ratio $\alpha = \lambda_{\text{IC}}/\lambda_\gamma$ is not a useful finite quantity for a pure $E0$ transition; $E0$ strengths are instead described by electronic factors and a nuclear monopole strength. The 691 keV 0^+ state of ^{72}Ge is the lecture's below-threshold conversion example [6, 14].

Caution

Do not use α without specifying the transition. It depends on Z, E_{tr}, shell, and multipolarity. Nor should an observed level half-life be identified with a photon partial half-life until all conversion and competing branches have been removed [6].

1.8 Nuclear recoil and resonant absorption (outline)

If the free nucleus is initially at rest and emits a photon of energy E_γ, momentum conservation requires nuclear recoil momentum $p = E_\gamma/c$. Non-relativistically,

$$E_R = \frac{p^2}{2M} = \frac{E_\gamma^2}{2Mc^2}, \tag{1.28}$$

so energy conservation gives

$$E_\gamma = E_0 - E_R \approx E_0 - \frac{E_0^2}{2Mc^2}, \tag{1.29}$$

where E_0 is the level difference. For absorption, the photon must supply $E_0 + E_R$. Free-nucleus emission and absorption lines are therefore separated by $\sim 2E_R$ (often eV scale), which can block resonance unless Doppler or natural widths overlap.

In a solid the recoil momentum can be taken by the crystal as a whole. The zero-phonon probability is finite and depends on temperature, gamma energy, and the lattice vibrational spectrum; it is not a sharp $E_R < \hbar\omega_{\text{phonon}}$ threshold. Recoilless emission and absorption constitute the **Mössbauer effect**, used for ultra-high-resolution nuclear spectroscopy [6, 14, 2].

Key idea

Students should remember:

- γ decay: same nucleus; $X^* \to X + \gamma$.
- Multipoles EL, ML; no $E0$ photon; no magnetic monopole.
- $|J_i - J_f| \le L \le J_i + J_f$, $L \ge 1$; $0 \to 0$ γ forbidden.
- Parity: EL has $\pi_f = \pi_i(-1)^L$; ML has $\pi_f = \pi_i(-1)^{L+1}$.
- $\lambda_\gamma \propto E_\gamma^{2L+1} B(\sigma L)$; Weisskopf units are benchmarks, not precision predictions.
- $\tau = 1/\lambda_{\text{tot}}$, $t_{1/2} = \tau \ln 2$, and $\Gamma = \hbar/\tau$.

- $\alpha = \lambda_{\mathrm{IC}}/\lambda_\gamma$ and $f_\gamma = 1/(1+\alpha)$; a pure $E0$ transition needs separate notation.

1.9 Deeper physics: multipoles, Weisskopf units, and conversion

1.9.1 Electric and magnetic multipole rates

An excited nuclear level can de-excite by emitting a photon of multipolarity σL ($\sigma = E, M$). In the long-wavelength limit the partial width scales as

$$\lambda_{\sigma L} \propto \frac{E_\gamma^{2L+1}}{(2L+1)!!}\,\frac{L+1}{L}\,|B(\sigma L)|^2, \tag{1.30}$$

where $B(EL)$ and $B(ML)$ are reduced transition probabilities [6, 1]. Selection rules follow from angular-momentum addition: an EL transition changes parity by $(-1)^L$, an ML transition by $(-1)^{L+1}$. The Weisskopf estimate replaces $|B(\sigma L)|^2$ by a single-particle value to define one "Weisskopf unit" (W.u.) [14].

Weisskopf estimate for an $E2$ transition

For a single-particle $E2$ transition with $E_\gamma = 0.5\,\mathrm{MeV}$ and $R \approx 5\,\mathrm{fm}$, the Weisskopf estimate gives a partial half-life of order $10^{-12}\,\mathrm{s}$ [6]. Measured $B(E2)$ values for collective rotational bands can exceed the Weisskopf value by tens to hundreds, signalling coherent motion of many nucleons. Conversely, $B(E2) \ll 1$ W.u. marks a hindered transition with poor radial overlap [14, 1].

1.9.2 Internal conversion as a competing channel

The same nuclear matrix element drives γ emission and internal conversion: an atomic electron carries away the transition energy instead of a photon. The total de-excitation rate includes a conversion coefficient α,

$$\lambda_{\mathrm{tot}} = \lambda_\gamma(1+\alpha), \tag{1.31}$$

so the observed photon intensity is reduced by $1/(1+\alpha)$ [6, 1]. Conversion dominates for low E_γ and high Z because the atomic electron can match the nuclear transition momentum near the nucleus. For a 100 keV $E2$ transition in $Z = 90$, α can exceed unity and most decays proceed without an observed γ [6, 34].

Key idea

From spectroscopy to reactions. Multipole selection rules constrain γ cascades following β or α decay and compound-nucleus evaporation (Lecture 21). A measured $B(E2)$ quantifies collectivity; a large α at low energy warns that photon intensities alone undercount the de-excitation rate [6, 20].

1.9.3 Angular correlations and mixed multipoles

When two successive γ rays are emitted from aligned nuclei, their angular correlation constrains the multipolarities and the mixing ratio δ between competing EL and ML amplitudes [6, 1]. Internal conversion competes with the same nuclear matrix element, so a γ-γ correlation analysis must include conversion branches that remove flux from the photon channel [34]. In compound-nucleus decay, the first emitted γ often carries the highest multipolarity allowed by angular-momentum selection, setting the pattern for subsequent statistical cascades analysed with Hauser–Feshbach theory (Lecture 21) [6, 14].

1.9.4 Collective $E2$ strength and rotational bands

Rotational bands in even–even nuclei exhibit a sequence of $E2$ transitions with similar $B(E2)$ values, often tens of W.u., signalling coherent quadrupole motion [14, 6]. The Weisskopf single-particle estimate is deliberately crude: it assumes one proton or neutron moving in a single orbit. Collective enhancement occurs when many nucleons contribute in phase. In reactions, Coulomb excitation of deformed targets populates the same $E2$ strength that γ spectroscopy measures in decay cascades (Lecture 21) [6, 2]. Conversion coefficients must still be applied when inferring $B(E2)$ from photon intensities alone.

Angular correlation coefficients and linear polarisation measurements assign multipolarities when conversion data are incomplete. Isomer traps and storage rings extend lifetime measurements into exotic regions where electronic timing is difficult. The nuclear clock theme shows that "γ decay" spans from mega-electronvolts down to electronvolts.

Physics-depth close

Selection rules, Weisskopf estimates, and conversion coefficients are the minimal toolbox for γ-ray spectroscopy. Isomers and the nuclear clock show that the same toolbox spans mega-electronvolts to electronvolts.

1.10 Further physics from the literature

1.10.1 What a measured lifetime actually determines

Suppose a level has gamma branches j, branching photon intensities $I_{\gamma j}$, and conversion coefficients α_j. The level half-life determines only the sum

$$\frac{\ln 2}{t_{1/2}} = \sum_j (1+\alpha_j)\lambda_{\gamma j}.$$

To extract $B(\sigma L)$ for one branch, the experimental analysis must (i) normalize the photon intensities, (ii) restore the unobserved conversion strength by multiplying branch j by $1+\alpha_j$, (iii) form its partial rate, and only then (iv) divide out the phase-space factor E_γ^{2L+1}. Confusing a level half-life with a photon partial half-life can produce a large error for a low-energy, high-Z transition [6, 1].

1.10.2 What one Weisskopf unit does and does not mean

One W.u. is the strength generated by a deliberately crude single-particle radial estimate. It provides a common scale across nuclei and energies, but it is not the statement that every one-particle transition has exactly that strength. A value far below one W.u. signals hindrance from configuration, isospin, or radial mismatch; a large $E2$ value often signals coherent collective motion. Basdevant emphasizes that collective quadrupole motion can make $E2$ transitions compete strongly even where a naive hierarchy would suggest otherwise [6, 1, 14].

1.10.3 A spectroscopy decision chain

No single observable usually supplies a complete assignment.

1. Level energies and coincidences establish the cascade.
2. Spin information restricts L through the triangle inequality.
3. Known parities select EL or ML for each L.
4. Angular correlations constrain L and the mixing ratio δ.
5. Linear polarization distinguishes electric from magnetic character.
6. Shell-resolved conversion coefficients $\alpha_K, \alpha_L, \ldots$ provide an independent multipolarity test.
7. A conversion-corrected partial lifetime yields $B(\sigma L)$, which can then be compared with a nuclear model.

This chain explains why selection rules by themselves identify possibilities, not measured amplitudes [6, 2, 20].

1.10.4 Internal conversion calculations

The nuclear matrix element is essentially common to gamma emission and conversion, so their ratio depends mainly on atomic structure, Z, transition energy, and multipolarity. Accurate coefficients require relativistic electron wave functions and finite nuclear size. Evaluated level schemes tabulate experimental or calculated shell coefficients; the rough Z^3 and inverse-energy trends are valuable intuition but should not replace those tables [6, 1, 20, 21].

1.10.5 Recoil, line width, and the Mössbauer limit

The free-nucleus recoil shift can exceed the natural width by many orders of magnitude even though it is tiny compared with E_γ. A solid can absorb momentum without creating a phonon, giving a zero-phonon line. Scanning source and absorber through resonance then resolves isomer shifts, electric quadrupole splittings, and magnetic hyperfine splittings. The 14.4 keV transition of ^{57}Fe is the standard example [6, 14, 2].

Reading guide

Krane [6], Ch. 10, and Dunlap [1], Ch. 10, give parallel derivations of multipole rates and conversion. Basdevant [14], Sec. 4.2, emphasizes matrix elements, collectivity, and conversion; Demtröder [2], Sec. 3.5, connects the long-wavelength ratio $R/\bar{\lambda}$ to lifetimes and recoil spectroscopy. The H. C. Verma *Nuclear Physics Fundamentals and Applications* sequence places “Gamma Decay” after its alpha- and beta-decay lectures and before nuclear reactions; that progression motivates the source-to-cascade narrative used here [32]. Evaluated numerical schemes belong to ENSDF/NuDat 3, with conversion coefficients from BrIcc when needed [20, 21, 34, 33].

1.10.6 Weisskopf estimates and conversion-corrected lifetimes

The total de-excitation rate of a level sums all γ and conversion channels. For branch j with multipolarity σL,

$$\frac{\ln 2}{t_{1/2}} = \sum_j (1 + \alpha_j)\, \lambda_{\gamma j}, \tag{1.32}$$

where $\lambda_{\gamma j} \propto E_{\gamma j}^{2L+1} |B(\sigma L)_j|^2$ [6, 1]. A Weisskopf estimate supplies a single-particle $|B(\sigma L)|^2$ for order-of-magnitude checks. If $\alpha_j \gg 1$, the level half-life is dominated by conversion even when the γ branch is invisible in a spectrum [34, 20].

Conversion correction for a $Z = 82$ transition

Consider an $M1$ transition at $E_\gamma = 100\,\mathrm{keV}$ in $Z = 82$. Tabulated α_K can exceed 10^3 for this combination [6, 34]. The measured level half-life then exceeds the photon partial half-life by the factor $1+\alpha \approx 10^3$. Quoting $B(M1)$ from the level lifetime without conversion correction would overestimate the nuclear matrix element by thirty orders of magnitude in rate.

1.10.7 From γ cascades to compound-nucleus decay

Compound-nucleus evaporation (Lecture 21) is a sequence of statistical γ and particle emissions. Each step obeys the same multipole and Hauser–Feshbach logic as discrete spectroscopy, but level densities replace resolved states [6, 1]. Fission fragments emit prompt γ rays before β decay (Lecture 24); stellar fusion chains terminate in γ emission from excited ^{4}He and CNO intermediates (Lecture 26) [36, 14]. Internal conversion competes most strongly at low E_γ and high Z, exactly where fission-fragment cascades are rich in low-energy transitions.

Key idea

Arc through the course. Multipole rules connect β-delayed γ spectroscopy (Lectures 18–19) to reaction-residue γ detection (Lecture 21) and fission-fragment decay heat (Lecture 24). Weisskopf units provide the first sanity check on any quoted $B(\sigma L)$ before invoking collectivity or hindrance [6, 14].

1.10.8 Mössbauer spectroscopy as the zero-recoil limit

When a nucleus in a solid emits a γ ray without recoil energy loss to lattice phonons, the natural line width is not Doppler-broadened by the free-nucleus recoil [6, 14]. The 14.4 keV transition in ^{57}Fe is the standard example: isomer shifts probe chemical environments, and quadrupole splitting maps local electric-field gradients. This is the same $E2/M1$ multipole language applied to condensed matter rather than to discrete level schemes in a decay chain. Recoil energy $E_{\text{rec}} = E_\gamma^2/(2Mc^2)$ is tiny compared with E_γ but enormous compared with eV-scale nuclear widths, which is why the Mössbauer condition requires a rigid lattice [2].

1.10.9 Isomer spectroscopy and K forbiddenness

Long-lived isomers in heavy and exotic nuclei often decay by hindered multipole transitions or by internal conversion when E_γ is small [6, 34]. K-isomers in deformed nuclei violate the selection rules for fast $E1$ decay because the projection quantum number K is not conserved in the available final states. Tracking arrays that record γ-γ coincidences apply the lecture selection rules event by event, filtering multipolarity before a level scheme is built [20, 51]. The ^{229}Th nuclear clock isomer at ~ 8 eV is an extreme case where conversion and radiative decay compete in a domain usually dominated by atomic physics [57].

1.11 Deeper reading: Weisskopf estimates, conversion, and isomers

Weisskopf single-particle estimates give reference lifetimes for EL and ML multipoles. Collective enhancement of $E2$ and K-forbidden hindrance of isomers are measured against those benchmarks. Internal conversion coefficients rise rapidly at low energy and high Z, so intensity balances in heavy nuclei require conversion tables, not γ counts alone.

The ^{229}Th nuclear clock isomer at ~ 8 eV pushes the same multipole ideas into the optical regime. Tracking arrays turn Lecture 20 selection rules into coincidence filters for constructing level schemes far from stability, linking back to collective structure (Lecture 15) and forward to reaction γ tagging (Lecture 21).

Weisskopf unit arithmetic

Compute a Weisskopf $E2$ lifetime for a 100 keV transition in a medium-mass nucleus and compare with a measured collective lifetime: the ratio is the enhancement factor. Repeat for an $M1$ single-particle estimate versus a hindered isomer. Those two ratios teach more than memorising selection-rule tables.

Internal conversion as a diagnostic

Conversion coefficient ratios α_K/α_L help assign multipolarity when angular distributions are unavailable. At very low energy, conversion can dominate emission entirely, which is why some isomers are detected via electrons or photons from subsequent atomic cascades.

Multipolarity decision tree

Given a transition energy, ΔI, and $\Delta\pi$, list the lowest allowed multipoles. Estimate Weisskopf lifetimes and decide whether the transition is likely prompt or isomeric. If Z is high and E is low, check conversion coefficients before predicting a γ branching ratio. This decision tree is exactly what analysis pipelines automate in tracking-array studies.

For the nuclear clock, note that an optical-energy nuclear transition blurs the line between atomic and nuclear spectroscopy: the multipole is still $M1$ (to leading order), but the engineering is laser physics. Lecture 20's selection rules remain the correct language even at $8\,\mathrm{eV}$.

Gamma spectroscopy turns selection rules into event filters. Weisskopf estimates and conversion coefficients remain the first tools for reading modern level schemes.

In practice, rework one numerical estimate from the lecture with a different parameter set and compare the shift to the quoted experimental uncertainty. If the shift exceeds the uncertainty, the estimate is teaching a scale, not delivering a fit. That distinction keeps theoretical cartoons honest when they sit beside evaluated data tables and modern many-body calculations. Along the course arc, write one sentence linking this chapter backward and one forward: the discipline of those two sentences is as important as any single formula. Examination problems rarely ask for a literature review, but they do ask for the scale argument that literature reviews presuppose.

Synthesis problem

Write a half-page note that (i) restates the chapter's central scale or selection rule in one equation, (ii) evaluates it numerically for one concrete nucleus or energy, and (iii) names the neighbouring lecture that uses the result. Keep the note free of research-frontier speculation; the goal is fluency with the lecture physics itself. If an assumption fails (Born approximation, spherical mean field, allowed transition, one-dimensional barrier), state the failure mode in a final sentence. That habit converts passive reading into examination-ready understanding and makes the later research-frontier box read as an extension rather than a replacement.

Research frontier: γ spectroscopy, isomers, and the nuclear clock

Multipole selection rules and internal conversion (Lecture 20) are everyday tools of modern γ-ray tracking arrays. Isomer spectroscopy of exotic and superheavy nuclei constrains deformation and K-forbiddenness, while conversion-coefficient evaluations (BrIcc) remain essential for intensity balances in complex decay schemes [34, 20]. A striking frontier is the ^{229}Th nuclear clock isomer: radiative decay of the $\sim 8\,\mathrm{eV}$ state has been observed, opening a path to a nucleus-based optical frequency standard and to tests of fundamental-constant drift [57]. Uncertainties that still matter include precise isomer energies and branching ratios in exotic nuclei, conversion-coefficient systematics at low energy, and the engineering path from a laboratory isomer observation to a closed-loop nuclear clock. The lecture's Weisskopf estimates and multipolarity diagnostics remain the first tools students use when reading modern γ-spectroscopy papers.

Beyond the thorium clock, isomer research with radioactive beams maps K-isomer lifetimes and hindered transitions that diagnose axial asymmetry and pairing. Tracking arrays that record γ-γ coincidences turn the lecture selection rules into event-by-event multipolarity filters, which is why modern papers still begin with angular-correlation and conversion arguments.

Student directions. (1) Weisskopf exercise: apply single-particle estimates to an $E2$ and an $M1$ transition of given energy and compare lifetimes. (2) Data lookup: using BrIcc or tables, find α_K for a 100 keV $E2$ in $Z = 50$ versus $Z = 90$. (3) Literature summary: summarise the ^{229}Th isomer energy measurement and why a nuclear clock could complement atomic clocks [57].

1.12 Problems with solutions

Problem 20.1: Multipole for $2^+ \to 0^+$

A nuclear transition proceeds from $J_i^\pi = 2^+$ to $J_f^\pi = 0^+$. List all multipoles allowed by angular momentum and parity, and identify the dominant one [6].

Solution 20.1

Step 1: Angular momentum.

$$|2 - 0| \le L \le 2 + 0 \quad \Rightarrow \quad L = 2.$$

Only quadrupole radiation is allowed.

Step 2: Parity. Both states have $\pi = +1$, so parity does not change. For $L = 2$,

$$EL: \ \pi_f = \pi_i(-1)^2 = \pi_i \quad \text{(allowed)}, \qquad ML: \ \pi_f = \pi_i(-1)^3 = -\pi_i \quad \text{(forbidden)}.$$

Step 3: Dominant multipole. The only allowed multipole is $E2$.

Problem 20.2: ^{117}In $1/2^- \to 9/2^+$

For $J_i^\pi = \frac{1}{2}^-$ to $J_f^\pi = \frac{9}{2}^+$, find allowed L values and the corresponding EL/ML assignments. Which multipole dominates? [6, 1]

Solution 20.2

Step 1:

$$\left|\tfrac{1}{2} - \tfrac{9}{2}\right| \le L \le \tfrac{1}{2} + \tfrac{9}{2} \quad \Rightarrow \quad L = 4, 5.$$

Step 2: Parity changes $(- \to +)$.

- $L = 4$: ML has $\pi_f = \pi_i(-1)^5 = -\pi_i \Rightarrow M4$. EL would preserve parity $\Rightarrow$ forbidden.
- $L = 5$: EL has $\pi_f = \pi_i(-1)^5 = -\pi_i \Rightarrow E5$. ML would preserve parity $\Rightarrow$ forbidden.

Step 3: Compare orders, not only electric versus magnetic character. The $E5$ amplitude contains one additional power of the small parameter kR, so its rate contains roughly an additional $(kR)^2$ suppression. That penalty overwhelms the usual enhancement of an electric multipole over a magnetic multipole of the same order. The dominant assignment is $M4$.

Problem 20.3: Why $0^+ \to 0^+$ cannot emit a photon

Show from the triangle inequality that a $0^+ \to 0^+$ transition cannot proceed by single-photon emission. What is the alternative electromagnetic channel? [6]

Solution 20.3

For $J_i = J_f = 0$,

$$|0 - 0| \leq L \leq 0 + 0 \quad \Rightarrow \quad L = 0.$$

A real photon multipole requires $L \geq 1$. Hence $\lambda_\gamma = 0$ for single-photon emission. The transition proceeds by internal conversion (electric monopole coupling to an atomic electron), or by e^+e^- pair creation if $E_{\text{tr}} > 1.022\,\text{MeV}$.

Problem 20.4: Conversion coefficient

A transition emits $N_\gamma = 8.0 \times 10^6$ photons and $N_e = 2.0 \times 10^6$ conversion electrons (all shells). Find α and the fraction of decays that proceed by photon emission [1].

Solution 20.4

$$\alpha = \frac{N_e}{N_\gamma} = \frac{2.0 \times 10^6}{8.0 \times 10^6} = 0.25.$$

Total electromagnetic decays $N_{\text{tot}} = N_\gamma + N_e = 1.0 \times 10^7$. Photon fraction:

$$\frac{N_\gamma}{N_{\text{tot}}} = \frac{1}{1 + \alpha} = \frac{1}{1.25} = 0.80 \quad (80\%).$$

Problem 20.5: Recoil energy

Estimate the nuclear recoil energy $E_R = E_\gamma^2/(2Mc^2)$ for the 662 keV γ ray of ^{137}Ba ($Mc^2 \approx 137 \times 931\,\text{MeV}$). Is E_R large compared with eV-scale chemical shifts? [6]

Solution 20.5

$$Mc^2 \approx 1.275 \times 10^5\,\text{MeV}, \qquad E_\gamma = 0.662\,\text{MeV}.$$

$$E_R = \frac{(0.662)^2}{2 \times 1.275 \times 10^5}\,\text{MeV} = \frac{0.438}{2.55 \times 10^5}\,\text{MeV} \approx 1.72 \times 10^{-6}\,\text{MeV} = 1.72\,\text{eV}.$$

Yes: E_R is of order eV, comparable to or larger than many chemical and hyperfine shifts, which is why free-atom resonant absorption is hindered and the Mössbauer (recoilless) effect is powerful in solids.

Problem 20.6: Assign $3^- \to 2^+$

List every allowed multipole for $3^- \to 2^+$, and identify the one normally expected to dominate [6, 1].

Solution 20.6

Angular momentum:

$$|3-2| \le L \le 3+2 \quad \Rightarrow \quad L = 1, 2, 3, 4, 5.$$

Parity changes. Lowest $L = 1$:

$$E1: \ \pi_f = \pi_i(-1)^1 = -\pi_i \quad \text{(allowed)}, \qquad M1: \ \text{parity unchanged (forbidden)}.$$

Applying the parity test to every L gives

$$E1, \ M2, \ E3, \ M4, \ E5.$$

The lowest member, $E1$, normally dominates because each higher order brings additional powers of kR. Structural hindrance can alter quantitative branching, so "dominant $E1$" is a Weisskopf-scale expectation, not an extra selection rule.

Problem 20.7: Isomeric hindrance

Explain qualitatively why an $M4$ isomer can have a half-life of minutes while a typical $E2$ state lives for picoseconds [6, 14].

Solution 20.7

Step 1: Why high L is costly. In the long-wavelength expansion a rank-L amplitude carries powers of $kR = E_\gamma R/\hbar c \ll 1$. Increasing L therefore strongly suppresses the squared amplitude, in addition to double-factorial factors.
Step 2: Compare energy dependences. The Weisskopf table gives $\lambda(M4) \propto E_\gamma^9$, whereas $\lambda(E2) \propto E_\gamma^5$, and magnetic radiation has an additional penalty at equal L. A low-energy $M4$ can therefore be slower by many orders of magnitude.
Step 3: Interpret the lifetime. Selection rules that force $M4$ can make the state isomeric. The exact lifetime cannot follow from a fixed "penalty per order" alone: A, E_γ, internal conversion, and the nuclear matrix element must also be specified.

Problem 20.8: Long-wavelength parameter

For $A = 125$ and $E_\gamma = 1.00\,\text{MeV}$, calculate R, kR, and the leading squared-amplitude penalty $(kR)^2$ for raising the multipole order by one. Explain why the complete Weisskopf ratio is not exactly $(kR)^2$ [6, 2].

Solution 20.8

Step 1: Radius.

$$R = 1.2A^{1/3}\,\text{fm} = 1.2(125)^{1/3}\,\text{fm} = 6.00\,\text{fm}.$$

Step 2: Expansion parameter.

$$kR = \frac{E_\gamma R}{\hbar c} = \frac{(1.00\,\text{MeV})(6.00\,\text{fm})}{197.327\,\text{MeV fm}} = 3.04 \times 10^{-2}.$$

Step 3: Rate scale.

$$(kR)^2 = 9.25 \times 10^{-4}.$$

The full ratio also contains different $(2L+1)!!$ factors, L-dependent coefficients, radial matrix elements, and electric or magnetic scales.

Problem 20.9: Weisskopf rate, lifetime, and width

For a 1.00 MeV $E2$ transition with $A = 100$, use

$$\lambda_{\text{W}}(E2) = 7.28 \times 10^7 A^{4/3} E_\gamma^5\ \text{s}^{-1}$$

to calculate the Weisskopf mean life, half-life, and natural width. If the measured partial half-life is 2.00 ps and conversion is negligible, estimate $B(E2)$ in W.u. [1].

Solution 20.9

Step 1: Weisskopf rate.

$$A^{4/3} = 100^{4/3} = 464.2, \qquad \lambda_{\text{W}} = 3.38 \times 10^{10}\,\text{s}^{-1}.$$

Step 2: Time scales.

$$\tau_{\text{W}} = \lambda_{\text{W}}^{-1} = 2.96 \times 10^{-11}\,\text{s}, \qquad t_{1/2,\text{W}} = \tau_{\text{W}} \ln 2 = 2.05 \times 10^{-11}\,\text{s}.$$

Step 3: Width.

$$\Gamma_{\text{W}} = \hbar\lambda_{\text{W}} = (6.5821 \times 10^{-16}\,\text{eV s})(3.38 \times 10^{10}\,\text{s}^{-1}) = 2.22 \times 10^{-5}\,\text{eV}.$$

Step 4: Strength in W.u. At fixed A, E_γ, L, the rate is proportional to $B(E2)$:

$$\frac{B(E2)}{B_{\text{W}}(E2)} = \frac{\ln 2/(2.00 \times 10^{-12}\,\text{s})}{3.38 \times 10^{10}\,\text{s}^{-1}} = 10.3\ \text{W.u.}$$

Problem 20.10: Conversion-corrected partial rate

A level decays through one electromagnetic transition with $t_{1/2} = 10.0\,\text{ns}$ and $\alpha = 3.00$. Find the total, photon, and conversion decay constants, the photon and electron fractions, and the total and photon partial widths [6, 1].

Solution 20.10

Step 1: Total rate.

$$\lambda_{\text{tot}} = \frac{\ln 2}{t_{1/2}} = 6.93 \times 10^7\,\text{s}^{-1}.$$

Step 2: Separate the channels.

$$\lambda_\gamma = \frac{\lambda_{\text{tot}}}{1+\alpha} = 1.73 \times 10^7\,\text{s}^{-1}, \qquad \lambda_{\text{IC}} = \alpha\lambda_\gamma = 5.20 \times 10^7\,\text{s}^{-1}.$$

Step 3: Fractions.

$$f_\gamma = \frac{1}{4} = 0.250, \qquad f_{\text{IC}} = \frac{3}{4} = 0.750.$$

Step 4: Widths.

$$\Gamma_{\text{tot}} = 4.56 \times 10^{-8}\,\text{eV}, \qquad \Gamma_\gamma = 1.14 \times 10^{-8}\,\text{eV}.$$

Using the level half-life directly as the photon partial half-life would overestimate the photon strength by $1 + \alpha = 4$.

Problem 20.11: Reading an angular correlation

A two-photon cascade has

$$W(\theta) = 1 + 0.20P_2(\cos\theta) - 0.05P_4(\cos\theta).$$

(a) Why is an unconditioned gamma ray from the same unpolarized source isotropic? (b) Evaluate $W(0^\circ)$ and $W(90^\circ)$. (c) What additional measurement distinguishes electric from magnetic character? [6]

Solution 20.11

Step 1: Origin of the axis. Before detecting the first photon, all magnetic substates are equally populated and no direction is preferred. Detection of γ_1 defines an axis and aligns the intermediate ensemble.

Step 2: Evaluate the Legendre polynomials. Since $P_2(1) = P_4(1) = 1$,

$$W(0^\circ) = 1 + 0.20 - 0.05 = 1.15.$$

Since $P_2(0) = -1/2$ and $P_4(0) = 3/8$,

$$W(90^\circ) = 1 - 0.10 - 0.05\left(\frac{3}{8}\right) = 0.88125.$$

Step 3: Electric or magnetic? Angular correlations constrain multipole order and mixing. A linear polarization measurement, commonly using polarization-dependent Compton scattering, distinguishes electric from magnetic character.

Problem 20.12: Dimensionless mixing ratio

An $M1 + E2$ transition has measured radiation-amplitude mixing ratio $\delta = -0.30$. Find the angle-integrated $M1$ and $E2$ fractions and explain what information is lost if only those fractions are reported.

Solution 20.12

$$f_{E2} = \frac{\delta^2}{1+\delta^2} = \frac{0.09}{1.09} = 0.0826, \qquad f_{M1} = \frac{1}{1+\delta^2} = 0.917.$$

The fractions contain δ^2, so they lose the negative relative phase. Angular-correlation or polarization interference terms retain the sign. A ratio of the bare $E2$ and $M1$ reduced matrix elements would not be a dimensionless replacement for δ.

Problem 20.13: BrIcc correction for $^{137\mathrm{m}}$Ba

Treat the 661.7 keV, $11/2^- \to 3/2^+$ transition as pure $M4$, and use the illustrative BrIcc value $\alpha_T = 0.11$. (a) Verify the leading multipole. (b) Find photon and conversion fractions. (c) If 10^6 isomers decay through this branch, estimate both yields [20, 21, 34].

Solution 20.13

$\Delta J = 4$ and parity changes; $M4$ is allowed and is lower order than the also-allowed $E5$. Therefore

$$f_\gamma = \frac{1}{1.11} = 0.901, \qquad f_{\mathrm{IC}} = \frac{0.11}{1.11} = 0.0991.$$

The expected yields are 9.01×10^5 photons and 9.91×10^4 conversion electrons before detector efficiencies. A precision result must use the shell sum and vacancy convention associated with the selected BrIcc record.

Bibliography

[1] R. A. Dunlap, *An Introduction to the Physics of Nuclei and Particles* (2nd ed.), IOP Publishing, Bristol (2023), DOI: 10.1088/978-0-7503-6094-4, Ch. 3 (Nuclear composition and size).

[2] W. Demtröder, *Nuclear and Particle Physics*, Undergraduate Lecture Notes in Physics, Springer, Cham (2023).

[3] S. Petrera, *Problems and Solutions in Nuclear and Particle Physics*, UNITEXT for Physics, Springer, Cham (2019).

[4] F. Terranova, *A Modern Primer in Particle and Nuclear Physics*, Oxford University Press (2021).

[5] S. D'Auria, *Introduction to Nuclear and Particle Physics*, Undergraduate Lecture Notes in Physics, Springer, Cham (2018).

[6] K. S. Krane, *Introductory Nuclear Physics*, Wiley, New York (1988).

[7] R. Hofstadter, "Electron scattering and nuclear structure," Rev. Mod. Phys. **28**, 214 (1956).

[8] H. F. Ehrenberg, R. Hofstadter, U. Meyer-Berkhout, D. G. Ravenhall, and S. E. Sobottka, "High-Energy Electron Scattering and the Charge Distribution of Carbon-12 and Oxygen-16," Phys. Rev. **113**, 666 (1959).

[9] H. Yukawa, "On the interaction of elementary particles. I," Proc. Phys.-Math. Soc. Japan **17**, 48 (1935).

[10] R. D. Woods and D. S. Saxon, "Diffuse surface optical model for nucleon-nuclei scattering," Phys. Rev. **95**, 577 (1954).

[11] H. G. J. Moseley, "The high-frequency spectra of the elements," Phil. Mag. **26**, 1024 (1913); **27**, 703 (1914).

[12] C. F. von Weizsäcker, "Zur Theorie der Kernmassen," Z. Phys. **96**, 431 (1935).

[13] P. Cappellaro, *Introduction to Applied Nuclear Physics* (MIT OpenCourseWare / LibreTexts), CC BY-NC-SA 4.0.

[14] J.-L. Basdevant, J. Rich, and M. Spiro, *Fundamentals in Nuclear Physics: From Nuclear Structure to Cosmology*, Springer, New York (2005).

[15] D. Tong, *Particle Physics*, Lecture notes (University of Cambridge / CERN school notes).

[16] M. G. Mayer, "On closed shells in nuclei. II," Phys. Rev. **75**, 1969 (1949).

[17] O. Haxel, J. H. D. Jensen, and H. E. Suess, "On the "magic numbers" in nuclear structure," Phys. Rev. **75**, 1766 (1949).

[18] T. Schmidt, "Über die magnetischen Momente der Atomkerne," Z. Phys. **106**, 358 (1937).

[19] L. W. Nordheim, "On spins, moments, and shells in nuclei," Phys. Rev. **78**, 294 (1950).

[20] Evaluated Nuclear Structure Data File (ENSDF), National Nuclear Data Center, Brookhaven National Laboratory, `https://www.nndc.bnl.gov/ensdf/`.

[21] NuDat 3, National Nuclear Data Center, Brookhaven National Laboratory, `https://www.nndc.bnl.gov/nudat3/`.

[22] N. J. Stone, "Table of nuclear magnetic dipole and electric quadrupole moments," At. Data Nucl. Data Tables **90**, 75 (2005); updated compilations at NNDC.

[23] W. N. Cottingham and D. A. Greenwood, *An Introduction to Nuclear Physics* (2nd ed.), Cambridge University Press, Cambridge (2001).

[24] H. Geiger and J. M. Nuttall, "The ranges of the α particles from the radioactive substances," Phil. Mag. **22**, 613 (1911).

[25] G. Gamow, "Zur Quantentheorie des Atomkernes," Z. Phys. **51**, 204 (1928).

[26] R. W. Gurney and E. U. Condon, "Wave mechanics and radioactive disintegration," Nature **122**, 439 (1928); Phys. Rev. **33**, 127 (1929).

[27] M. Wang, W. J. Huang, F. G. Kondev, G. Audi, and S. Naimi, "The AME 2020 atomic mass evaluation (II). Tables, graphs and references," Chin. Phys. C **45**, 030003 (2021).

[28] Laboratoire National Henri Becquerel (LNHB), Recommended decay data, `http://www.lnhb.fr/nuclear-data/nuclear-data-table/`.

[29] L. M. Langer, R. D. Moffat, and H. C. Price, Jr., "Low energy beta-ray spectra: P^{32} and Cu^{64}," Phys. Rev. **76**, 1725 (1949).

[30] L. M. Langer and H. C. Price, Jr., "Shapes of the beta-spectra of the forbidden transitions of Sb^{124}, Rb^{86}, Sr^{89}, Y^{91}, and Cs^{137}," Phys. Rev. **75**, 1769 (1949).

[31] D. C. Camp and L. M. Langer, "The shape of the ^{66}Ga positron spectrum and the contribution from $0^+ \to 0^+$ transitions," Phys. Rev. **129**, 1782 (1963).

[32] H. C. Verma, *Nuclear Physics: Fundamentals and Applications*, NPTEL/IIT Kanpur lecture series, `https://hcverma.in/ncl_phy_lectures`.

[33] International Atomic Energy Agency, *LiveChart of Nuclides*, evaluated structure, decay, reaction, and fission-yield data, `https://www-nds.iaea.org/relnsd/vcharthtml/VChartHTML.html`.

[34] T. Kibédi, T. W. Burrows, M. B. Trzhaskovskaya, P. M. Davidson, and C. W. Nestor, Jr., "Evaluation of theoretical conversion coefficients using BrIcc," Nucl. Instrum. Methods Phys. Res. A **589**, 202 (2008), DOI: 10.1016/j.nima.2008.02.051.

[35] D. A. Brown *et al.*, "ENDF/B-VIII.0: The 8th major release of the nuclear reaction data library with CIELO-project cross sections, new standards and thermal scattering data," Nucl. Data Sheets **148**, 1 (2018), DOI: 10.1016/j.nds.2018.02.001.

[36] B. Acharya *et al.*, "Solar fusion III: New data and theory for hydrogen-burning stars," Rev. Mod. Phys. **97**, 035002 (2025), DOI: 10.1103/8lm7-gs18.

[37] S. N. Ghoshal, "An experimental verification of the theory of compound nucleus," Phys. Rev. **80**, 939 (1950), DOI: 10.1103/PhysRev.80.939.

[38] D. Adhikari *et al.* (PREX Collaboration), "Accurate determination of the neutron skin thickness of ^{208}Pb through parity-violation in electron scattering," Phys. Rev. Lett. **126**, 172502 (2021), DOI: 10.1103/PhysRevLett.126.172502.

[39] B. T. Reed, F. J. Fattoyev, C. J. Horowitz, and J. Piekarewicz, "Implications of PREX-II on the equation of state of neutron-rich matter," Phys. Rev. Lett. **126**, 172503 (2021), DOI: 10.1103/PhysRevLett.126.172503.

[40] B. Hu *et al.*, "Ab initio predictions link the neutron skin of ^{208}Pb to nuclear forces," Nature Phys. **18**, 1196 (2022), DOI: 10.1038/s41567-022-01715-8.

[41] E. Epelbaum, H.-W. Hammer, and U.-G. Meißner, "Modern theory of nuclear forces," Rev. Mod. Phys. **81**, 1773 (2009), DOI: 10.1103/RevModPhys.81.1773.

[42] H.-W. Hammer, S. König, and U. van Kolck, "Nuclear effective field theory: Status and perspectives," Rev. Mod. Phys. **92**, 025004 (2020), DOI: 10.1103/RevModPhys.92.025004.

[43] T. Otsuka, A. Gade, O. Sorlin, T. Suzuki, and Y. Utsuno, "Evolution of shell structure in exotic nuclei," Rev. Mod. Phys. **92**, 015002 (2020), DOI: 10.1103/RevModPhys.92.015002.

[44] H. Hergert, S. K. Bogner, T. D. Morris, A. Schwenk, and K. Tsukiyama, "The in-medium similarity renormalization group: A novel ab initio method for nuclei," Phys. Rep. **621**, 165 (2016), DOI: 10.1016/j.physrep.2015.12.007.

[45] J. M. Lattimer and M. Prakash, "The equation of state of hot, dense matter and neutron stars," Phys. Rep. **621**, 127 (2016), DOI: 10.1016/j.physrep.2015.12.005.

[46] J. M. Lattimer, "Neutron stars and the nuclear matter equation of state," Annu. Rev. Nucl. Part. Sci. **71**, 433 (2021), DOI: 10.1146/annurev-nucl-102419-124827.

[47] B. P. Abbott *et al.* (LIGO Scientific Collaboration and Virgo Collaboration), "GW170817: Observation of gravitational waves from a binary neutron star inspiral," Phys. Rev. Lett. **119**, 161101 (2017), DOI: 10.1103/PhysRevLett.119.161101.

[48] M. J. Dolinski, A. W. P. Poon, and W. Rodejohann, “Neutrinoless double-beta decay: Status and prospects,” Annu. Rev. Nucl. Part. Sci. **69**, 219 (2019), DOI: 10.1146/annurev-nucl-101918-023407.

[49] M. Agostini, G. Benato, J. A. Detwiler, J. Menéndez, and F. Vissani, “Toward the discovery of matter creation with neutrinoless $\beta\beta$ decay,” Rev. Mod. Phys. **95**, 025002 (2023), DOI: 10.1103/RevModPhys.95.025002.

[50] P. Gysbers *et al.*, “Discrepancy between experimental and theoretical β-decay rates resolved from first principles,” Nature Phys. **15**, 428 (2019), DOI: 10.1038/s41567-019-0450-7.

[51] H. L. Crawford, K. Fossez, S. König, and A. Spyrou, “A vision for the science of rare isotopes,” Annu. Rev. Nucl. Part. Sci. **74**, 141 (2024), DOI: 10.1146/annurev-nucl-121423-091501.

[52] Nuclear Science Advisory Committee, *A New Era of Discovery: The 2023 Long Range Plan for Nuclear Science*, U.S. Department of Energy and National Science Foundation (2023), `https://nuclearsciencefuture.org/`.

[53] S. A. Giuliani, Z. Matheson, W. Nazarewicz, E. Olsen, P.-G. Reinhard, J. Sadhukhan, B. Schuetrumpf, N. Schunck, and P. Schwerdtfeger, “Colloquium: Superheavy elements: Oganesson and beyond,” Rev. Mod. Phys. **91**, 011001 (2019), DOI: 10.1103/RevModPhys.91.011001.

[54] N. Schunck and D. Regnier, “Theory of nuclear fission,” Prog. Part. Nucl. Phys. **125**, 103963 (2022), DOI: 10.1016/j.ppnp.2022.103963.

[55] I. Counts, J. Hur, D. P. L. Aude Craik, H. Jeon, C. Leung, J. C. Berengut, A. Geddes, A. Kawasaki, W. Jhe, and V. Vuletić, “Evidence for nonlinear isotope shift in Yb^+ search for new boson,” Phys. Rev. Lett. **125**, 123002 (2020), DOI: 10.1103/PhysRevLett.125.123002.

[56] I. Angeli and K. P. Marinova, “Table of experimental nuclear ground state charge radii: An update,” At. Data Nucl. Data Tables **99**, 69 (2013), DOI: 10.1016/j.adt.2011.12.006.

[57] S. Kraemer *et al.*, “Observation of the radiative decay of the ^{229}Th nuclear clock isomer,” Nature **617**, 706 (2023), DOI: 10.1038/s41586-023-05894-z.